Measurement and Modelling of Radiative Coupling in Oscillator Arrays

Robert A. York, *Member, IEEE*, and Richard C. Compton, *Member, IEEE*

Abstract—**Arrays of coupled oscillators can be used for power-combining at microwave and millimeter-wave frequencies, and have been successfully demonstrated with a variety of devices. Such arrays have also recently been mode-locked for pulse generation, and can be configured for phase-shifterless beam-scanning. The nonlinear theory of coupled-oscillator phase dynamics depends crucially on the parameters describing the coupling between oscillators. Methods for experimental characterization of these parameters are described here, and simple models are developed which reproduce the measurements quite well. The models apply to radiative coupling and the effects of external reflectors which are sometimes used for stabilization. The theory is verified with a two-oscillator system.**

I. Introduction

THE INCREASING demand for high power, high efficiency solid-state sources in the millimeter-wave range has spurred interest in new technologies for power-combining, using quasi-optical techniques [1]–[2]. In a quasi-optical power-combining array, a large number of devices are integrated in a planar radiating structure, and the power-combining takes place in free-space. Such arrays can accomodate a large number of devices for high-power generation, and very high combining efficiencies are possible.

One of the earliest reported quasi-optical power-combiners used a small array of coupled-oscillators, where each oscillator was connected to a patch antenna, and mutual coupling between the antennas induced mutual injection-locking [3]. A circuit analysis of such "interjection-locked" arrays was described at about the same time [4]. Since then, the coupled-oscillator array concept has been further developed, and arrays using Gunn diodes and FETs have been successfully demonstrated [5]–[7]. In addition, arrays of coupled millimeter-wave sources have been found to possess other interesting and potentially useful properties, such as mode-locking for pulse generation [8]–[9], and phase-shifterless beam-scanning [4]. These arrays are inherently suited to monolithic integration, and will find application in systems where compact and lightweight components are required.

In a previous paper [5], a theory describing the nonlinear dynamics of oscillator arrays was derived and used to examine the existence and stability of various modes of the system, which are characterized by a common frequency and particular phase relationship amongst the oscillators. It was found that the strength and phase angle of the mutual coupling has a profound effect on the steady-state solution, and therefore it is important to accurately characterize these parameters. This paper describes the measurement and modelling of radiative coupling in quasi-optical oscillator arrays. Two different mutual coupling mechanisms are identified, and it is shown that a very simple model adequately reproduces the experimental observations for some cases of practical interest, using common active patch oscillator circuits [5], [6], [17].

Manuscript received March 30, 1992; revised July 20, 1992. This work was supported by the U.S. Army Research Office.

R. A. York is with the Department of Electrical Engineering, University of California at Santa Barbara, Santa Barbara, CA 93106.

R. C. Compton is with the School of Electrical Engineering, Cornell University, Ithaca, NY 14853.

IEEE Log Number 9205452.

II. Coupled Oscillator Theory

The theory of coupled oscillators has attracted considerable attention in recent years, as it appears to model many diverse natural phenomena quite well [10]–[11]. Through this research it has been learned that the system dynamics are not greatly influenced by the particular nonlinearities within each oscillator, provided this nonlinearity is sufficient to produce sinusoidal oscillations [11]. This allows us to select the simplest possible model for each oscillator. A popular choice is the Van der Pol model [12], which can be derived by representing the device by a lumped negative resistance (conductance) embedded in a series (parallel) resonant circuit. The impedance of the device depends nonlinearly on the amplitude of oscillation. To ensure nearly sinusoidal oscillations near the resonant frequency of the embedding circuit, it is assumed that the Q-factor is at least $Q > 10$. Allowing for the possibility of an externally injected signal V_{inj}, the sinusoidal Van der Pol model can be written as

$$\frac{dV}{dt} = V\left[\frac{\mu\omega_0}{2Q}(A_0^2 - |V|^2) + j\omega_0\right] + \frac{\omega_0}{2Q}V_{inj} \tag{1}$$

where μ is a device-dependent nonlinearity parameter, V is the complex output voltage of the oscillator, Q is the Q-factor of the embedding circuit, and A_0 and ω_0 are the free-running ($V_{inj} = 0$) amplitude and frequency,

To extend this model to a system of coupled oscillators, we assume that the mutual interaction between oscillators i and j in the system can be described by a complex coupling coefficient, written as

$$\kappa_{ij} \equiv \lambda_{ij} \exp(-j\Phi_{ij})$$

In most arrays, reciprocity will hold so that $\kappa_{ij} = \kappa_{ji}$. In a system of N oscillators, the injected signal at the ith oscillator will be

$$V_{inj} = \sum_{j=1}^{N} \kappa_{ij} V_j$$

where V_j represents the output signal of the jth oscillator. Note that κ_{ii} (the self-interaction term) is not necessarily zero—this will be discussed later. Using this expression and the Van der Pol model (1), a set of coupled, nonlinear differential equations describing the amplitude and phase dynamics of the system have been derived [9]. If the mutual coupling between oscillators is not too strong, then we can ignore the amplitude dynamics and concentrate our attention on the phase dynamics. For a system of N oscillators with free-running frequencies ω_i and free-running amplitudes A_i, the phase distribution will evolve in time according to [5, 9]

$$\frac{d\theta_i}{dt} = \omega_i - \frac{\omega_i}{2Q}\sum_{j=1}^{N}\lambda_{ij}\frac{A_j}{A_i} \cdot \sin(\Phi_{ij} + \theta_i - \theta_j) \qquad i = 1, 2, \cdots, N \qquad (2)$$

where θ_i is the instantaneous phase of oscillator i (and hence $d\theta_i/dt$ represents the instantaneous frequency). Under certain conditions all of the oscillators can become synchronized to a common frequency ω, so that $d\theta_i/dt = \omega$ for all i. Furthermore, the phase relationship between all oscillators will remain constant in this locked state, and so we write $\theta_i - \theta_j = \phi_i - \phi_j$, where the ϕ_i are time-independent constants describing the relative phase distribution in the steady-state, and can be found by solving

$$\omega = \omega_i \left[1 - \sum_{j=1}^{N}\frac{\lambda_{ij}}{2Q}\frac{A_j}{A_i}\sin(\Phi_{ij} + \phi_i - \phi_j)\right] \qquad i = 1, 2, \cdots, N \qquad (3)$$

Noting that one of the phase variables is arbitrary and can be set to zero, we see that for a given set of free-running and coupling parameters there are generally 2^{N-1} different sets of phases, or modes, which satisfy (3) in the steady-state. However, few of these modes are stable. Mode stability can be analyzed using a perturbation analysis [5], [13], in which (2) is linearized around some particular solution. If $\hat{\theta}$ is a solution vector of (2), we perturb this solution by a small amount $\theta_i = \hat{\theta}_i + \delta_i$, and find an evolution equation for the δ_i as

$$\frac{d\delta_i}{dt} = -\frac{\omega_i}{2Q}\sum_{j=1}^{N}\lambda_{ij}\frac{A_j}{A_i}(\delta_i - \delta_j) \cdot \cos(\Phi_{ij} + \hat{\theta}_i - \hat{\theta}_j) \qquad i = 1, 2, \cdots, N \qquad (4)$$

which can be written as a matrix equation

$$\frac{d}{dt}[\delta] = [M][\delta] \qquad (5)$$

where M is an $N \times N$ matrix. One of the eigenvalues of this matrix will have a zero real part, since one of the phase variables is arbitrary. In order that the perturbation δ not grow without bound, the remaining eigenvalues of M must have negative real parts [13]. This additional constraint is usually restrictive enough to remove all but one of the solutions to (3). Limited space in this paper does not permit elaboration on the important topic of mode stability, and this will be discussed in a future paper. The above analysis is sufficient for what follows.

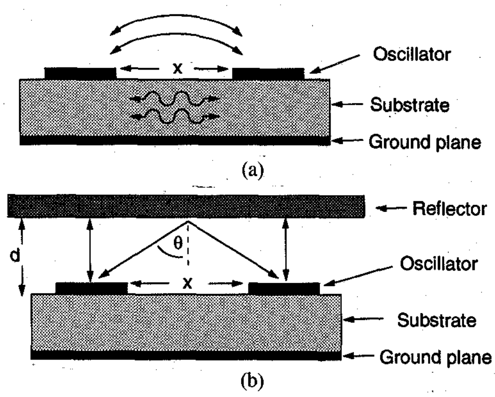

Fig. 1. Two classes of radiative coupling in oscillator arrays. (a) Free-space and surface-wave coupling, which are nearly always present. (b) Quasi-optical reflector, forming a Fabry-Perot cavity. The reflector affects the inter-oscillator coupling and also the behavior of each individual oscillator in the absence of coupling. Both types can be accounted for with simple models.

III. Coupling Mechanisms and Measurement

From (2) it is clear that both the magnitude and phase of the coupling coefficient, κ_{ij}, will have an important influence on the phase dynamics of the system. In a typical oscillator array this mutual coupling can take several forms. Two of these are almost always present in planar radiating arrays: free-space interactions, and coupling through surface-waves propagating in the dielectric substrate (Fig. 1(a)). The latter is significant for electrically thick substrates. These radiative coupling mechanisms have been characterized both theoretically and experimentally for many types of planar radiators, such as the patch antenna [14]–[15]. The strength and phase of this interaction is a strong function of the element separation. This is not always desirable in an oscillator array, since the element spacing also determines the radiation pattern of the array and hence cannot be set arbitrarily.

Another important situation is depicted in Fig. 1(b), where the array is placed in an open quasi-optical cavity. Open resonators can have very high Q-factors, and hence are useful for frequency stabilization. The particular cavity shown in Fig. 1(b) is created by the partially reflecting mirror (such as a dielectric sheet) and the ground plane of the array. The individual oscillators couple to a set of cavity modes, which are the vehicle for interaction [1]. This type of coupling can thus be controlled by the reflectivity, shape, and position of the mirror. Alternative coupling schemes can also be used, such as a planar transmission-line circuit for adjacent oscillators. The latter is a more flexible design alternative than the proximity coupling scheme, however it may be undesirable if substrate real-estate is scarce. In the remainder of this paper we restrict our attention to the radiative coupling schemes shown in Fig. 1.

An elegantly simple technique has in fact already been described for the experimental characterization of free-space

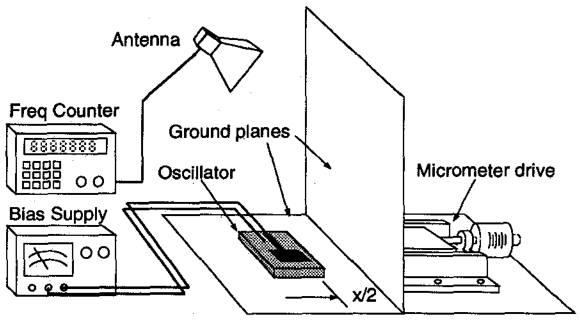

Fig. 2. Setup for coupling measurements. A vertical ground plane images a single oscillator, simulating two identical coupled oscillators. The oscillation frequency is then monitored while the metal sheet is moved away from the oscillator. This shift is related to the coupling coefficient in (7).

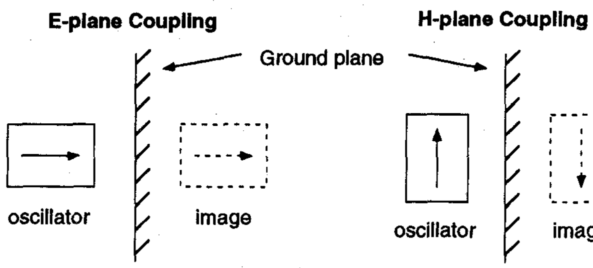

Fig. 3. Illustration of the imaging of an oscillator in the two principal radiation planes, for linearly polarized antennas. The arrow indicate the direction of current on the planar antennas.

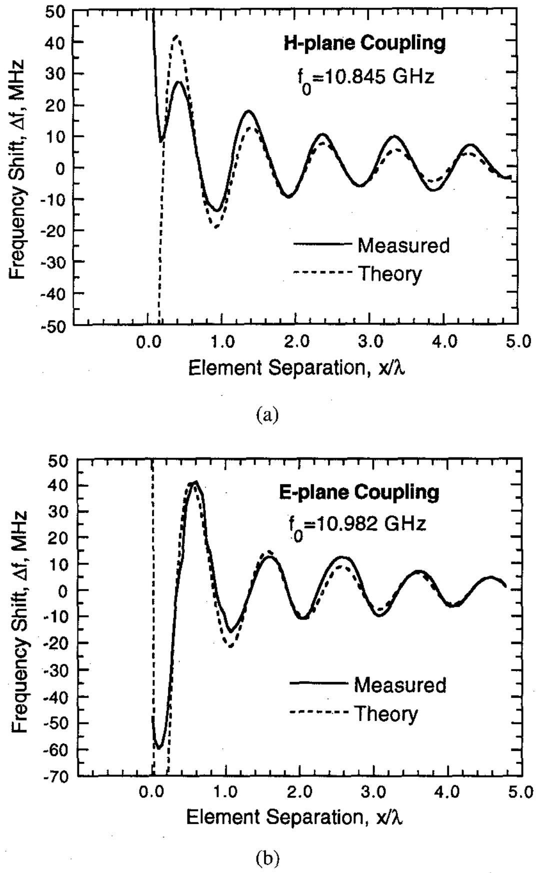

Fig. 4. Measured frequency shift versus oscillator separation (in wavelengths) for (a) H-plane coupling, and (b) E-plane coupling. An X-band Gunn diode/patch antenna oscillator was used. The theory curve is calculated using the simple model (8) as described in the text.

oscillator coupling [16]. As shown in Fig. 2, a single planar oscillator is imaged by a ground plane, thus simulating two identical, coupled oscillators. The coupling is controlled by adjusting the spacing between the oscillator and the mirror. As the mirror position is changed, the output frequency of the system also changes, and this frequency shift can be related to the coupling coefficient through equations (3). For two identical, frequency-locked oscillators (i.e., $\omega_1 = \omega_2 \equiv \omega_0, A_1 = A_2$) with $\kappa_{21} = \kappa_{12} = \lambda \exp(-\jmath\Phi)$ and $\kappa_{11} = \kappa_{22} = 0$, (3) gives, in the steady-state,

$$\omega = \omega_0\left[1 - \frac{\lambda}{2Q}\sin(\Phi + \Delta\phi)\right]$$
$$\omega = \omega_0\left[1 - \frac{\lambda}{2Q}\sin(\Phi - \Delta\phi)\right] \quad (6)$$

where $\Delta\phi = \phi_2 - \phi_1$, the relative phase difference between the two oscillators. Depending on the orientation of the two oscillators, either in-phase or out-phase oscillators are simulated in this technique, as illustrated in Fig. 3 for an oscillator with a linearly polarized antenna. For both cases, either of equations (6) can be used to get

$$\frac{\Delta f}{f_0} = \pm\lambda'(x)\sin\Phi(x) \quad (7)$$

where $\lambda' = \lambda/2Q$ and $\Delta f = f - f_0$. The frequency shift is thus a function of the coupling coefficient only, which in turn is a function of the oscillator separation x as indicated in (7). The plus-sign applies for H-plane coupling ($\Delta\phi = \pi$), while the minus-sign applies for E-plane coupling ($\Delta\phi = 0$). Equation (7) is similar in form to (9) in [21], which was derived by other methods.

Two typical experimental results are shown in Fig. 4 for an active patch antenna with an integrated X-band Gunn diode [6], [16]. In each of the graphs a theoretical curve has been plotted for comparison. These have been calculated using a simple model in which the coupling signal is described by the far-field approximation for the antenna. In this approximation the field strength is proportional to $1/r$, where r is the distance from the antenna. The phase of the signal is calculated using the free-space propagation constant, $k_0 = \omega_0/c$, where c is the speed of light. Near-field effects can be partially accounted for with an additional phase term, φ, which is empirically determined [21]. If x is taken as the oscillator separation, this simple model for the free-space coupling is written as

$$\lambda'(x) = \frac{C}{k_0 x} \quad \text{and} \quad \Phi(x) = k_0 x + \varphi \quad (8)$$

where C and φ are fitted parameters and are dependent on the polarization of the coupling. For our active patch design, the experimental curves in Fig. 4 were found to be well described by

$$\text{E-plane:} \quad C = 0.013 \quad \varphi = 60^\circ$$
$$\text{H-plane:} \quad C = 0.010 \quad \varphi = -80^\circ$$

This simple model appears to work quite well for element spacings of a half-wavelength or more (a similar conclusion was reached in [21]). Note also that for typical array spacings of $x < \lambda$, the measurements indicate that significant mutual coupling will exist beyond nearest neighbors. However, it is possible that the nearest neighbors could effectively screen outlying oscillators and reduce this influence. Thus far, theoretical predictions based on nearest-neighbor coupling have compared very favorably with array measurements; these results will be presented in a future paper.

The excellent agreement for the simple model above suggests that a similar description of the coupling due to a partially reflecting mirror might be possible. In this case, the interaction is modelled as a simple plane-wave reflection from the mirror, which is governed by the Fresnel equations [18]. This is depicted by arrows in Fig. 1(b) for a flat sheet reflector (multiple reflections are ignored). If we define the path length $l = 2\sqrt{d^2 + (x/2)^2}$, where d is the distance between the reflector and the oscillator array, then the simple coupling model is

$$\lambda'(x,d) = \frac{C|\Gamma(\theta)G(\theta)|}{k_0 l} \quad \text{and}$$
$$\Phi(x,d) = k_0 l + \varphi + \angle\Gamma(\theta) \tag{9}$$

where $\Gamma(\theta)$ is the complex reflection coefficient of the reflector, which is a function of the angle of incidence $\theta = \tan^{-1}(x/2d)$ as well as the orientation of the oscillators (polarization of the field). $G(\theta)$ is the relevant gain function (E- or H-plane) of the antenna. Again, C and φ are empirically determined quantities. A corollary of this model is that each oscillator will also receive a portion of its own output signal, which is reflected directly back from the mirror. Such "self-injection-locking" is governed by Adler's equation [19], which reduces to an equation of the form (7). This self-interaction term is modelled by a nonzero κ_{ii}, which we allowed for in writing (2).

To explore the validity of this approach, experiments were performed using a single active patch oscillator, with a 1 inch thick dielectric sheet reflector ($\epsilon_r = 4.0$) mounted on an adjustable stand above the array. A typical measurement of the frequency variation versus reflector position for an X-band oscillator is shown in Fig. 5. The theory curve is calculated using the simple model (9), with $x = \theta = 0$, and follows the measurements surprisingly well. This is a useful result, considering the alternative methods for modelling the effects of external reflectors. Rigorously, the presence of the reflector affects the driving-point impedance of the antenna, and this in turn forces a change in the oscillator frequency. This driving point impedance can be calculated by a straightforward but lengthy and computationally expensive mode-matching procedure [1]. The simple model presented here will be especially useful in computer simulations of array dynamics, where computational efficiency is important.

In summary, mutual coupling in oscillator arrays with the (optional) presence of a reflector can be modelled as a superposition of three effects: a direct signal from the neighboring oscillator (8), a signal from the neighbor due to the reflector (9), and the self-injection-locking described above. Depending on the particular reflector used and/or the proximity of neighboring oscillators, one of these effects may dominate the others.

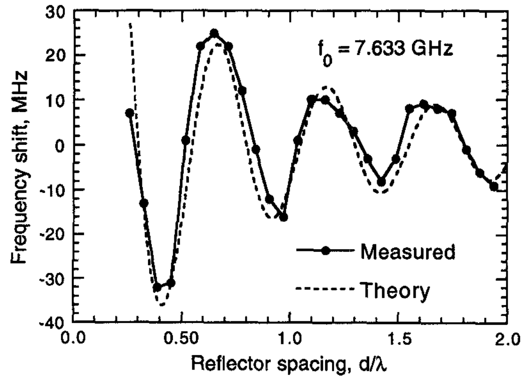

Fig. 5. Frequency shift as a dielectric slab (1" thick, $\epsilon_r = 4$) is moved above a Gunn/patch oscillator operating at 7.635 GHz. The effects of the reflector can be described by including a "self-interaction" term in the coupled-oscillator theory, and can be modelled by a simple expression.

IV. Two Coupled, Nonidentical Oscillators

The simplest application of the coupled-oscillator theory and coupling models described above is for the case of two coupled oscillators. This is also one of the few situations in which an exact analytical result can be found, and has been considered by various authors using many different techniques [21]–[23]. We will consider two oscillators which interact by direct, free-space mechanisms, as described by (8). Two simultaneous equations must be solved, which are found from (3) as

$$\begin{aligned} \omega &= \omega_1 \left[1 - \lambda' \frac{A_2}{A_1} \sin(\Phi - \Delta\phi)\right] \\ \omega &= \omega_2 \left[1 - \lambda' \frac{A_1}{A_2} \sin(\Phi + \Delta\phi)\right] \end{aligned} \tag{10}$$

The steady-state phase-shift which satisfies (10) is found as

$$\Delta\phi = 2\tan^{-1}\left[\frac{a \pm \sqrt{a^2 + b^2 - \Delta\omega^2}}{b + \Delta\omega}\right] \tag{11}$$

where

$$\begin{aligned} a &= \lambda' \cos\Phi(\omega_2 A_1/A_2 + \omega_1 A_2/A_1) \\ b &= \lambda' \sin\Phi(\omega_2 A_1/A_2 - \omega_1 A_2/A_1 \end{aligned}$$

and thus there are two possible solutions for this system. The solutions of (10) are subject to the stability condition

$$\left[\omega_2 \frac{A_1}{A_2}\cos(\Phi + \Delta\phi) + \omega_1 \frac{A_2}{A_1}\cos(\Phi - \Delta\phi)\right] > 0 \tag{12}$$

and this determines the proper sign in (11). The synchronized frequency can then be found by substituting back into (10). In the case of instantaneous coupling ($\Phi = 0$) this equation

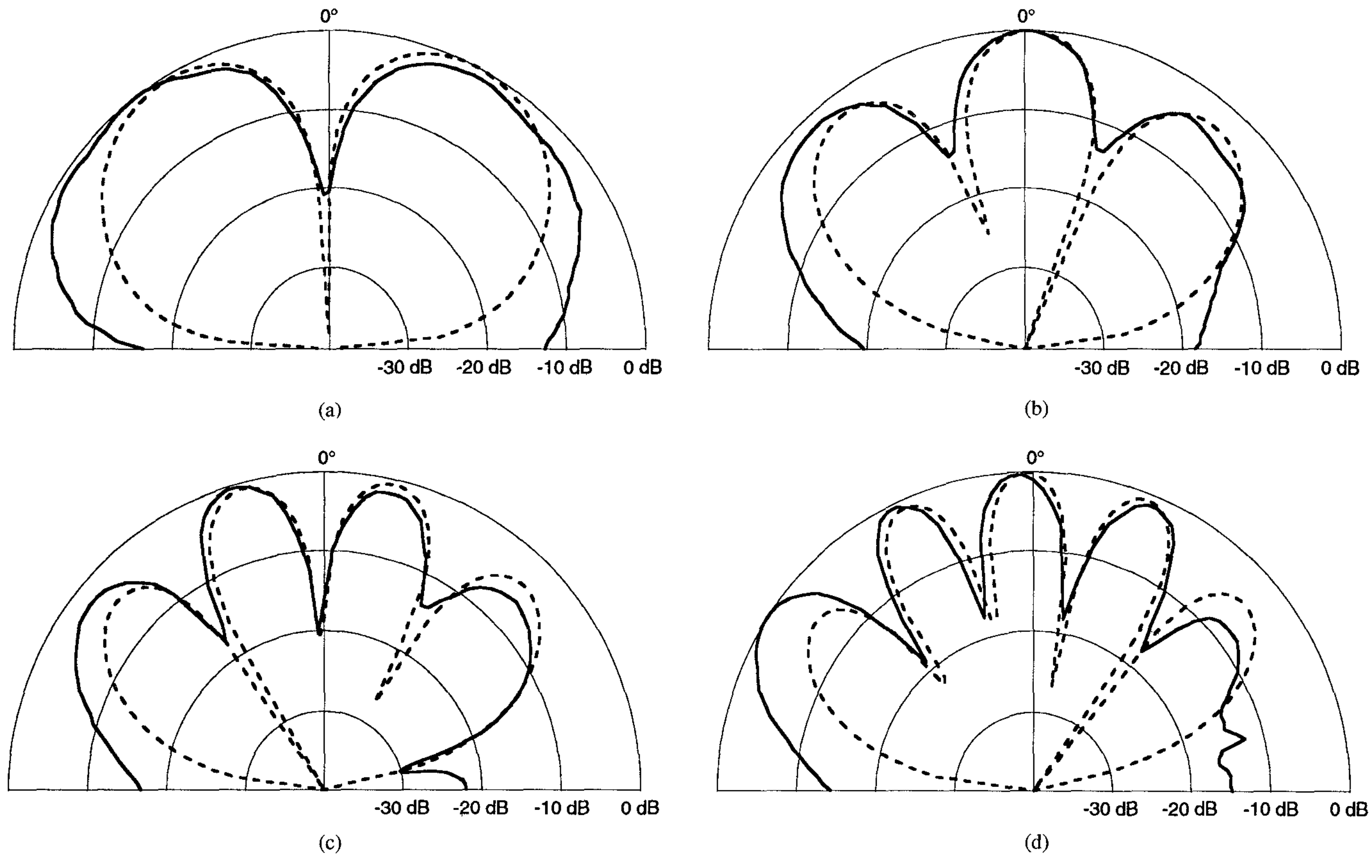

Fig. 6. A selection of radiation patterns for the two-oscillator system, with different oscillator separations. (a) $x = 15$ mm, (b) $x = 30$ mm, (c) $x = 45$ mm, and (d) $x = 60$ mm. Solid line is the measured pattern, and the dotted line is theory. The oscillators had measured free-running frequencies of approximately 10.8 GHz, and similar amplitudes. Good agreement in the placement of lobes and nulls indicate an accurate prediction of the phase shift.

reduces to

$$\sin \Delta\phi = \frac{\omega_2 - \omega_1}{\lambda' \left(\omega_1 \frac{A_2}{A_1} + \omega_2 \frac{A_1}{A_2} \right)}$$

$$\omega = \omega_1 \omega_2 \frac{\frac{A_1}{A_2} + \frac{A_2}{A_1}}{\omega_1 \frac{A_2}{A_1} + \omega_2 \frac{A_1}{A_2}}$$

which is the same result derived previously by Kaplan and Radparvar [22].

To illustrate the behaviour of the system, consider the case of two oscillators with identical free-running parameters, $\omega_1 = \omega_2$ and $A_1 = A_2$. Equations (11) and (12) become

$$\cos \Phi \sin \Delta\phi = 0 \quad \text{and}$$
$$\cos \Phi \cos \Delta\phi > 0$$

giving the solution

$$\Delta\phi = \begin{cases} 0, & -\pi/2 < \Phi < \pi/2 \\ \pi, & \pi/2 < \Phi < 3\pi/2 \end{cases}$$

and thus the two modes of operation are either in-phase or out-of-phase. This would be clearly evident from a measurement of the radiation pattern.

This theory was tested with a two-oscillator array, using an X -band active patch oscillator as described previously. The first step involved an experimental determination of the parameters C and φ in (8). The oscillators were then mounted on adjustable carrier so that the spacing and hence coupling could be continuously varied. The array was constructed for H-plane coupling. Several radiation pattern measurements were performed for different element spacings, and a few of these are shown in Fig. 6. The measurements support the theoretical observation of two distinct modes, which are approximately in-phase or out-of-phase. For each case the free-running parameters of each oscillator were carefully measured, and this information, along with the coupling model (8), was used to predict the final frequency and phase shift. Theoretical radiation patterns have been plotted for comparison in Fig. 6, with excellent agreement theory and experiment regarding the number and placement of lobes and nulls. Discrepancies in magnitude, especially at large angles from broadside, are a result of using a simplified patch antenna radiation model [20] for the theoretical pattern.

The measured radiation patterns were used to find the actual phase shift between the oscillators, and the differences between theory and experiment for all of the measurements has been plotted versus oscillator spacing in Fig. 7. The differences between theory and experiment for the oscillation frequency are also shown. This figure clearly shows that the simple coupling model (8) and the oscillator array theory (2) accurately describe the physical situation, except at small element separations. At such small element spacings, the far-field approximation used in (8), and the assumption of weak

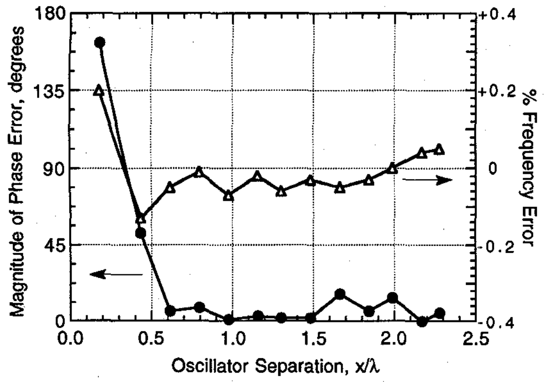

Fig. 7. Comparison of theory and experiment for both frequency and phase in the two oscillator system. Solid dots indicate the magnitude of the difference between theoretical and experimental phase shifts. Open triangles indicate the percent discrepancy between predicted and measured output frequency of the system. Good agreement is observed for spacings on the order of a half-wavelength or more.

coupling used in (2), are no longer valid. In such cases the coupling parameters can be found empirically, and oscillator amplitude dynamics must be accounted for [9].

V. Conclusions

A successful theory of coupled-oscillator arrays relies on a description of both the individual oscillators and the mechanics of interelement coupling. Using a theory based on the Van der Pol oscillator and a previously described imaging technique, mutual coupling between microwave oscillators can be experimentally determined. It was found that a very simple model for direct, radiative coupling between oscillators can be fitted to experimental data, and that subsequent predictions based on this model are accurate for oscillator separations of a half-wavelength or more. This model was extended to account for the external reflecting elements which are sometimes used in quasi-optical cavities. This led to the introduction of a "self-interaction" term, which accounts for the effects of the reflector on a single oscillator. The coupled-oscillator theory and radiative models were tested with two nonidentical oscillators, and very good agreement was observed between theory and experiment. The models developed here will be instrumental in future simulations of large array dynamics, where computational efficiency is paramount.

Acknowledgment

The authors wish to acknowledge Dr. Jim Mink at ARO for his support and encouragement, and Professors D. B. Rutledge at Caltech and K. D. Stephan at U. Mass. for helpful discussions and advice. The authors also thank the reviewers for many constructive comments.

References

[1] J. W. Mink, "Quasi-optical power combining of solid-state millimeter-wave sources," *IEEE Trans. Microwave Theory Tech.*, vol. MTT-34, pp. 273–279, Feb. 1986.
[2] J. C. Wiltse and J. W. Mink, "Quasi-optical power combining of solid-state sources," *Microwave J.*, pp. 144–156, Feb. 1992.
[3] R. J. Dinger, D. J. White, and D. R. Bowling, "10 GHz space power-combiner with parasitic injection-locking," *Electron. Lett.*, vol. 23, pp. 397–398, 9 Apr. 1987.
[4] K. D. Stephan, "Inter-injection-locked oscillators for power combining and phased arrays," *IEEE Trans. Microwave Theory Tech.*, vol. MTT-34, pp. 1017–1025, Oct. 1986.
[5] R. A. York and R. C. Compton, "Quasi-optical power-combining using mutually synchronized oscillator arrays," *IEEE Trans. Microwave Theory Tech.*, vol. 39, pp. 1000–1009, June 1991.
[6] K. Chang, K. A. Hummer, and J. L. Klein, "Experiments on injection-locking of active antenna elements for active phased arrays and spatial power combiners," *IEEE Trans. Microwave Theory Tech.*, vol. 37, pp. 1078–1084, July 1989.
[7] J. Birkeland and T. Itoh, "A 16 element quasi-optical FET oscillator power combining array with external injection locking," *IEEE Trans. Microwave Theory Tech.*, vol. 40, pp. 475–481, Mar. 1992.
[8] R. A. York and R. C. Compton, "Mode-locked oscillator arrays," *IEEE Microwave Guided-Wave Lett.*, vol. 1, pp. 215–218, Aug. 1991.
[9] ——, "Experimental observation and simulation of mode-locking in coupled-oscillator arrays," *J. Appl. Phys.*, vol. 71, no. 6, pp. 2959–2965, Mar. 15, 1992.
[10] S. H. Strogatz and R. E. Mirollo, "Phase-locking and critical phenomena in lattices of coupled nonlinear oscillators with random intrinsic frequencies," *Physica D*, vol. 31, pp. 143–168, 1988.
[11] N. Koppel, "Toward a theory of modelling central pattern generators," in *Neural Control of Rythmic Movements in Vertebrates*, ch. 10, A. H. Cohen, Ed., New York: Wiley, 1988.
[12] B. Van der Pol, "The nonlinear theory of electric oscillations," *Proc. IRE*, vol. 22, pp. 1051–1085, Sept. 1934.
[13] S. Wiggins, *Introduction to Nonlinear Dynamical Systems and Chaos*. Springer: Berlin, 1990.
[14] D. M. Pozar, "Input impedance and mutual coupling of rectangular microstrip antennas," *IEEE Trans. Antennas Propagat.*, vol. AP-30, pp. 1191–1196, Nov. 1982.
[15] R. P. Jedlicka, M. T. Poe, and K. R. Carver, "Measured mutual coupling between microstrip antennas," *IEEE Trans. Antennas Propagat.*, vol. AP-29, pp. 147–149, Jan. 1981.
[16] W. P. Shillue and K. D. Stephan, "A technique for the measurement of mutual impedance of monolithic solid-state quasi-optical oscillators," *Microwave and Optical Tech. Lett.*, Dec. 1990.
[17] H. J. Thomas, D. L. Fudge, and G. Morris, "Gunn source integrated with microstrip patch," *Microwaves & RF*, pp. 87–89, Feb. 1985.
[18] S. Ramo, J. R. Whinnery, T. Van Duzer, *Fields and Waves in Communication Electronics*, 2nd Ed., New York: Wiley, 1984.
[19] K. Kurokawa, "Injection-locking of solid-state microwave oscillators, *Proc. IEEE*, vol. 61, pp. 1386–1409, Oct. 1973.
[20] J. R. James, P. S. Hall, and C. Wood, *Microstrip Antenna Theory and Design*. London: Peter Peregrinus Ltd., 1981, pp. 77–80.
[21] K. D. Stephan and S. L. Young, "Mode Stability of radiation-coupled interinjection-locked oscillators for integrated phased arrays," *IEEE Trans. Microwave Theory Tech.*, vol. 36, pp. 921–924, May 1988.
[22] B. Z. Kaplan and K. Radparvar, "Canonic coupling of sinusoidal oscillators: New results," *Int. J. Systems Sci.*, vol. 16, pp. 1257–1263, 1985.
[23] V. P. Rubanik, "Mutual Synchronization of Self-Oscillating Systems," *Radio. Eng. Electron. Phys.*, vol. 7, pp. 1584–1592, Oct. 1962.

Robert A. York (S'86–M'91) received the B.S. degree in electrical engineering from the University of New Hampshire in 1987, and the M.S. and Ph.D. degrees in electrical engineering from Cornell University in 1989 and 1991, respectively.

In November 1991 he joined the faculty of Electrical and Computer Engineering at the University of California at Santa Barbara. His group at UCSB is currently involved with the design and fabrication of millimeter and sub-millimeter-wave devices, quasi-optical device arrays and nonlinear or non-reciprocal components, and quasi-optical measurement techniques.

Dr. York is a member of the Compound Semiconductor Research Group (CO-SEARCH) at UCSB. His other research interests include microwave materials measurements, and developing CAD methods for educational purposes. He was recipient of a 1990 MTT-S Graduate Fellowship Award, and co-recipient of the Ban Dasher award for Best Paper at the 1989 IEEE Frontiers in Education Conference.

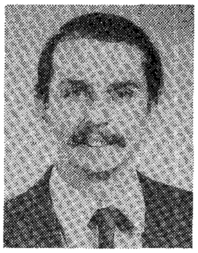

Richard C. Compton (S'84–M'87) received the B.Sc. from the University of Sydney in 1983.

During his Ph.D., at the California Institute of Technology (1983–1987), he worked as a Fulbright scholar on several projects, including the design, fabrication, and measurement of millimeter and submillimeter-wave antennas and arrays. He co-developed an interactive microwave CAD education package *Puff,* which is used in microwave classes at universities worldwide. His group at Cornell University is working in the area of millimeter-wave integrated circuit design and fabrication, and techniques for testing circuits at millimeter wavelengths.

Dr. Compton has been a consultant for the Hughes Aircraft Company, and TRW. He is a National Science Foundation Presidential Young Investigator, has served as an Editor for the *IEEE Antennas and Propagation Magazine,* and is currently an Associate Editor for the IEEE TRANSACTIONS ON EDUCATION.